

Genetic capsid modifications allow efficient re-targeting of adeno-associated virus type 2

ANNE GIROD¹, MARTIN RIED¹, CHRISTIANE WOBUS², HARALD LAHM¹, KRISTIN LEIKE¹,
JÜRGEN KLEINSCHMIDT², GILBERT DELÉAGE³ & MICHAEL HALLEK^{1,4}

¹Laboratorium für Molekulare Biologie, Genzentrum and ⁴Medizinische Klinik III, Klinikum Großhadern, Ludwig-Maximilians-Universität München, Feodor-Lynen-Straße 25, D-81377 München, Germany

²Deutsches Krebsforschungszentrum, Forschungsschwerpunkt Angewandte Tumorstudiologie, Im Neuenheimer Feld 242, D-69120 Heidelberg, Germany

³Pôle BioInformatique Lyonnais, Laboratoire de Conformation des Protéines, Institut de Biologie et Chimie des Protéines, UPR412-CNRS, F-69367 Lyon Cedex 07, France

Correspondence should be addressed to M.H.; email: hallek@lmb.uni-muenchen.de

The human parvovirus adeno-associated virus type 2 (AAV2) has many features that make it attractive as a vector for gene therapy^{1,2}. However, the broad host range of AAV2 might represent a limitation for some applications in vivo, because recombinant AAV vector (rAAV)-mediated gene transfer would not be specific for the tissue of interest. This host range is determined by the binding of the AAV2 capsid to specific cellular receptors and/or co-receptors³⁻⁶. The tropism of AAV2 might be changed by genetically introducing a ligand peptide into the viral capsid, thereby redirecting the binding of AAV2 to other cellular receptors. We generated six AAV2 capsid mutants by inserting a 14-amino-acid targeting peptide, L14, into six different putative loops of the AAV2 capsid protein identified by comparison with the known three-dimensional structure of canine parvovirus. All mutants were efficiently packaged. Three mutants expressed L14 on the capsid surface, and one efficiently infected wild-type AAV2-resistant cell lines that expressed the integrin receptor recognized by L14. The results demonstrate that the AAV2 capsid tolerates the insertion of a nonviral ligand sequence. This might open new perspectives for the design of targeted AAV2 vectors for human somatic gene therapy.

To specifically modify the natural tropism of AAV2, a detailed analysis of the three-dimensional structure of the viral capsid would be very useful. However, the three-dimensional structure of AAV2 is unknown. Moreover, previous genetic analyses of AAV2 mutants did not determine capsid regions mediating the binding of AAV2 to its natural receptor⁷⁻⁹. Therefore, we developed a hypothetical model of the AAV2 capsid three-dimensional structure based on the following assumptions: AAV2 is homologous in its structure to other parvoviruses; its tropism is determined by non-conserved amino acids; and the region allowing the insertion of polypeptides for AAV2 re-targeting should be hydrophilic and flexible. To derive some structural information on the AAV2 capsid protein, we analyzed the known three-dimensional structure of the canine parvovirus (CPV) capsid protein¹⁰ using the SOPM algorithm¹¹ and aligned the AAV2 and CPV capsid protein amino acid sequences with the CLUSTAL W program¹². Using this approach, we identified six sites in the AAV2 capsid protein, residues 261, 381, 447, 534, 573 and 587 (Fig. 1), that were expected to accept the insertion of a ligand polypeptide without disruption of functions essential for the viral life cycle.

To re-target AAV2, we inserted the 14-amino-acid peptide L14 (QAGTFALRGDNPQG) into the *cap* gene at these six sites. We chose L14, which has the RGD motif of the laminin fragment P1 (ref. 13), because it is the target for several cellular integrin receptors¹³ and can also serve as viral receptor¹⁴; no specific secondary structure of L14 is required for recognition of the receptor¹³; and L14 has been used successfully for re-targeting avian retroviruses¹⁵.

We first analyzed the six AAV2 capsid mutants (I-261, I-381, I-447, I-534, I-573 and I-587) for their ability to package the viral genome. There was no quantitative or qualitative difference between the mutants and wild-type AAV2 in the production of duplex monomer and dimer replicative forms of AAV2 during packaging in HeLa cells (data not shown). Moreover, each mutant could be efficiently packaged (Table 1). We confirmed the particle concentrations by electron microscopy (data not shown).

To determine whether the structure of the capsid mutants was similar to that of wild-type AAV2, we did an ELISA (enzyme-linked immunosorbent assay) using the A20 monoclonal antibody, which specifically reacts with completely assembled AAV2 capsids¹⁶. A20 reacted with capsid mutants I-447, I-534, I-573 and I-587, but not with mutants I-261 and I-381, indicating that both the capsid assembly and the A20 epitope were conserved in four of the six mutants (Table 1).

We next determined whether the L14 peptide would be exposed on the surface of the capsid mutants. For this, we did two different ELISAs using a polyclonal antibody against L14 (Fig. 2a). In the first, direct ELISA, viral particles were directly attached to microtiter plates, and the reactivity of the capsids

Table 1 Capsid formation of the AAV2 capsid mutant virions

virus	particles/mla	A20+capsids/mlb
wt AAV2	8×10^{13}	6×10^{12}
I-261	1×10^{12}	- ^c
I-381	1×10^{12}	- ^c
I-447	1×10^{13}	8×10^{11}
I-534	5×10^{11}	3×10^{10}
I-573	1×10^{12}	1×10^{117}
I-587	4×10^{13}	3×10^{12}

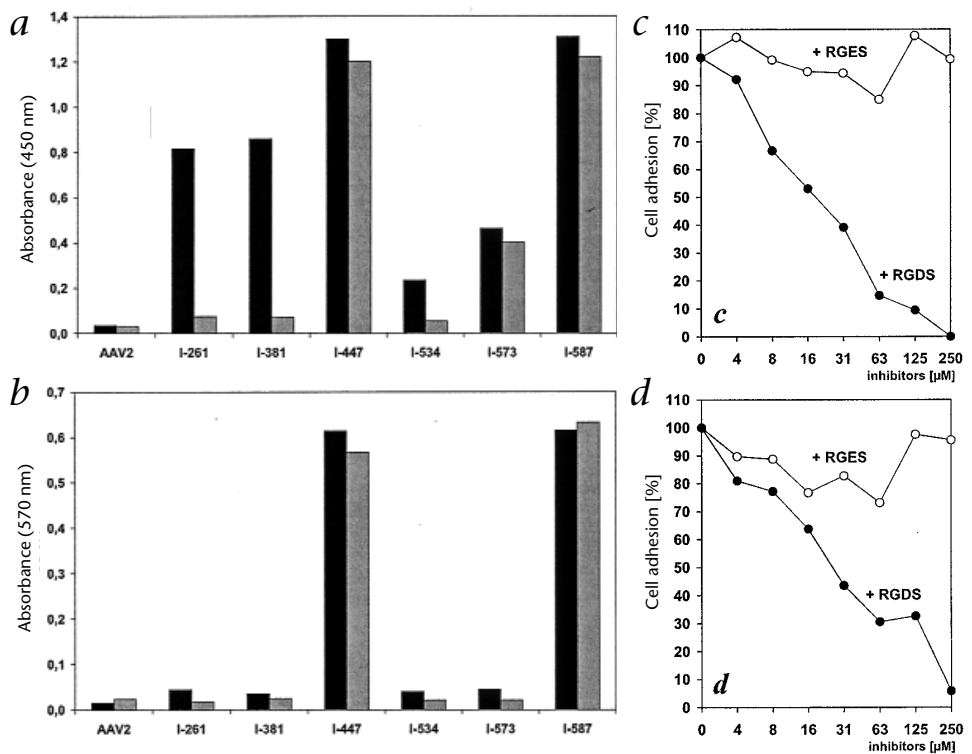
^aTiters of particles with an AAV2 genome. ^bTiters of particles showing the conformational A20 epitope. ^cNo A20 epitope could be detected on the capsid.

ARTICLES

Fig. 2 Presentation and functionality of the L14 sequence. **a**, Detection of L14 on the capsid surface of the mutants by either a direct ELISA (filled bars) or an indirect ELISA (shaded bars). **b**, Attachment assays of B16F10 (■) and RN22 (□) cells on the different viral preparations. The number of adherent cells was measured by a colorimetric assay and is given as absorbance. **c** and **d**, Inhibition assays of the attachment of B16F10 cells on mutants I-447 (**c**) and I-587 (**d**). Inhibitors: RGDS (●) and RGES (○). **a–d**, Data represent one of three independent similar experiments.

In B16F10 cells, Rep was expressed after infection with I-587 (Fig. 3) but not I-447. The titer of I-587 was estimated as high as 1×10^6 Rep-expression-forming units (EFU)/ml (Table 2). Similar results were obtained with RN22 cells (data not shown). In addition, by using a rAAV(I-587)/*LacZ* vector containing the *LacZ* reporter gene in a modified capsid presenting the L14 peptide at site 587, we demonstrated the feasibility of targeted gene transfer in B16F10 cells (Fig. 3c). The titer of rAAV(I-587)/*LacZ* was 5×10^4 *LacZ*-EFU/ml, representing an increase of the susceptibility of B16F10 cells for rAAV vectors by more than 4,000% (Table 2).

The attachment of AAV to its host cell seems to be a two-step mechanism that requires heparan sulfate proteoglycan as a primary receptor for the attachment of AAV to the cell membrane⁴ and either $\alpha V\beta 5$ integrin⁵ or human fibroblast growth factor receptor molecule⁶ as co-receptors. To determine the relative con-



tributions of heparan sulfate proteoglycan and L14-specific integrin receptor for infecting B16F10 cells with I-587, cells were infected in the presence of either 100 μ g/ml soluble heparin, a specific inhibitor of the AAV–heparan sulfate proteoglycan interaction⁴, or 200 μ M RGDS blocking peptide (Table 2). Transduction of Co-115 cells with rAAV/*LacZ* and rAAV(I-587)/*LacZ* was inhibited by more than 99% by heparin. In contrast, infection of B16F10 cells by rAAV(I-587)/*LacZ* could not be blocked by heparin but could be blocked by RGDS peptide, indicating that the mutant I-587 infected B16F10 cells through the L14-specific integrin receptor without the contribution of heparan sulfate proteoglycan (Table 2).

Re-targeting of AAV2 has been attempted using different strategies. One attempt added the single-chain fragment variable region of a monoclonal antibody against CD34 to the N terminus of the VP2 capsid protein¹⁸. Although re-targeted AAV2 virions were obtained that were able to infect CD34⁺ cells, this strategy had two chief disadvantages. The infectious titer was relatively low (4×10^2 virions per ml). Moreover, because the method of virus production required all three wild-type capsid proteins (VP1, VP2 and VP3) in addition to the single-chain fragment variable-VP2 fusion protein, the final vector preparation contained both wild-type and re-targeted rAAV capsids. Another approach to re-targeting AAV2 used bispecific antibodies recognizing the AAV2 viral capsid (through one Fab arm) and the alternative cell surface receptor (through the other Fab arm)¹⁹. This strategy allowed the transduction of megakaryocytic leukemia cell lines through the vector–bispecific antibody complex. However, the success of this approach depends on a very stable

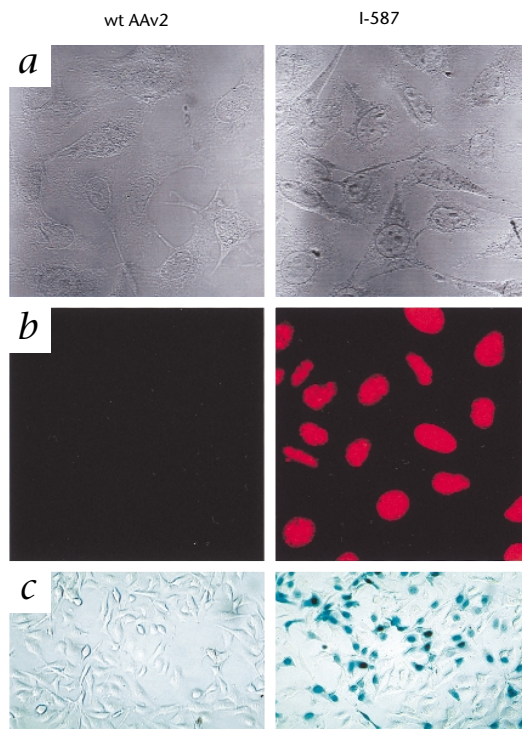


Fig. 3 Transduction of B16F10 cells. **a** and **b**, B16F10 cells infected with wild-type AAV2 (wt AAV2) or with mutant I-587 and visualized with light microscopy (**a**) or Rep-immunofluorescence staining (**b**). Original magnification, $\times 63$. **c**, X-gal staining of B16F10 cells infected with rAAV/*LacZ* or rAAV(I-587)/*LacZ*. Original magnification, $\times 20$.

interaction between the vector particle and the bispecific antibodies to prevent premature dissociation of the targeting antibody from the vector particle. Moreover, the use of bispecific antibodies might require an additional purification step to remove free antibody from the viral preparation and to avoid competition of free antibody with virus-bispecific antibody complexes for the cellular receptor.

In conclusion, our study represents the first successful attempt, to our knowledge, of insertional mutagenesis of the capsid protein for re-targeting the viral tropism of AAV2 to cells that are normally resistant to AAV2 infection. This indicates that a genetic receptor targeting of AAV2 vectors is possible and opens new avenues for the design of targeted AAV2 vectors for human somatic gene therapy, in particular for *in vivo* protocols.

Methods

Capsid protein structure analysis. All protein sequence analyses were done on the World-Wide Web by NPS[®] (Network Protein Sequence analysis, URL: <http://pbil.ibcp.fr/NPSA>). The CPV VP2 capsid protein (protein data bank code, 2CAS) related to AAV2 was found by scanning the NRL-3D database using the Smith and Waterman algorithm²⁰. The observed secondary structure of the CPV VP2 capsid protein was derived from crystallographic data by using the classical DSSP algorithm²¹ on the 2CAS file of atomic coordinates (Fig. 1a, row 1). The predicted secondary structure of the same protein was determined by the SOPM method¹¹ (Fig. 1a, row 2). The comparison of both observed and predicted secondary structures yielded a prediction accuracy level of about 84% (472 correctly predicted residues over 563 residues), indicating that the SOPM algorithm provided very precise results for this protein family. Thus, the sequence of the corresponding capsid protein of AAV2, VP3, was subjected to the same SOPM algorithm (Fig. 1a, row 3). The comparison of the predicted secondary structures for both protein sequences (CPV VP2 and AAV2 VP3) indicated that both proteins had similar topologies, allowing the use of the CPV capsid protein structure as a crude template for the AAV2 capsid protein. After analysis of the three dimensional structure of the CPV VP2 capsid protein with the RASMOL program, six regions in this protein were identified that were exposed on the viral capsid surface and were expected to be flexible enough to accept the insertion of a peptide sequence (Fig. 1b). The corresponding regions on the AAV2 VP3 capsid protein were identified by alignment of the sequences of the CPV VP2 capsid protein and the corresponding capsid protein of AAV2, VP3 (Fig. 1c). We excluded the possibility that the delineated sites for insertion were not predicted as regular secondary structure elements of the AAV2 capsid protein (Fig. 1a), where insertions would destabilize the capsid.

Plasmids. The plasmid pUC-AV2 was constructed by subcloning the 4.8-kb *Bgl*III fragment of pAV2 (37216; ATCC, Rockville, Maryland) into the *Bam*HI site of the pUC19 (New England Biolabs) by blunt-end ligation. It contains the full-length AAV2 genome and served as the parental plasmid to all constructs described in this report.

The plasmid pCap was obtained by blunt-end subcloning the 2.2-kb *Eco*RI-*Bsp*MI fragment of pUC-AV2 into the *Eco*RI site of the pUC19; therefore, it contains only the *cap* gene. It served as template for all PCR reactions.

The plasmids pl-261, pl-381, pl-447, pl-534, pl-573 and pl-587 contain the full-length AAV2 genome; the L14-encoding sequence was inserted in the *cap* gene of the AAV2 genome after nucleotides 2985, 3345, 3543, 3804, 3921 and 3963, respectively (Fig. 1c, precise location in the capsid protein sequence). The mutagenesis was achieved by using the ExSite[™] PCR-based Site-Directed Mutagenesis Kit as described by the supplier (Stratagene, La Jolla, California). For each mutant, a PCR fragment was generated by using the pCap plasmid as the template with two primers: one (K) containing the 20 nucleotides belonging to the *cap* gene immediately upstream of the insertion site and also some nucleotides coding for the 5' extremity of the L14 peptide; and the other (L) containing the 20 nucleotides belonging to the *cap* gene immediately downstream of the insertion site and also some nucleotides coding for the 3' extremity of the L14 peptide. The PCR products were amplified into bacteria and sequenced. The 1.4-kb *Eco*NI-*Xcm*I fragment containing the L14-encoding sequence was then subcloned in pUC-AV2 from which the corresponding fragment encoding the wild-type *cap* sequence had been removed. The following primers were used: K/261 (5'-CTTGGGAAATTTGTTGTAGAGGT-3') and L/261 (5'-CCGGCACTTTTGCCTCCGCGGTGATAATCCACAAGGAAGC-

CAATCAGGAGCCTCGAA-3') for pl-261; K/381 (5'-CTTGGTTC-AGGGTGAGGTATCCAT-3') and L/381 (5'-CCGGCACTTTTGCCC-TC-CCGGTGATAATCCACAAGGAAACGGGAGTCCAGGAGT-3') for pl-381; K/447 (5'-CTTGTCTGCTCAAGTAATACAGGT-3') and L/447 (5'-CCGGCACTTTTGCCTCCGCGGTGATAATCCACAAGGAAACAACTC-CAAGTGGAAAC-3') for pl-447; K/534 (5'-CTTGAATACTTTT-CTTCATCG-3') and L/534 (5'-CCGGCACTTTTGCCTCCGCGGTGATAATCCACAAGGACCTCA-GAGCGGGTTCAT-3') for pl-534; K/573 (5'-CTTGCCTAGC-CACGGGATTGGTT-3') and L/573 (5'-CCGGCACTTTTGC-CTCCGCGGTGATAATCCACAAGGAGCAGTATGGTTCTGTATC-3') for pl-573; and K/587 (5'-CTTGGTTCCTCTCTGGAGGT-3') and L/587 (5'-CCGGCACTTTTGCCTCCGCGGTGATAATCCACAAGGAAGA-CAAGCAGCTACCGAGA-3') for pl-587.

The pRC plasmid was constructed by blunt-end subcloning of the 4.5-kb *Xba*I-*Xba*I fragment of psub201(+) (ref. 22; plasmid obtained from R.J. Samulski) into the *Pst*I and *Bam*HI sites of the pSV40oriAAV (ref. 23).

The pRC(I-587) plasmid was a derivative of the pRC plasmid, obtained after subcloning of the *Eco*NI-*Xcm*I fragment of pl-587 in pRC from which the corresponding fragment had been removed. Both plasmids pRC and pRC(I-587) contain the AAV2 *rep*- and *cap*-encoding regions but lack the viral ITRs; therefore, they allow the production of helper-free AAV2-based vectors either in a wild-type AAV2 capsid (pRC) or in a capsid presenting the L14 peptide at the residue 587 (pRC(I-587)).

The pZnL plasmid was constructed by inserting the *Bgl*III fragment of pAD-*LacZ* (plasmid obtained from A. Doenecke) into the *Sna*BI-*Sna*BI sites of the psub201(+). The resulting plasmid is an AAV2-based vector plasmid with the *zeocin* selectable marker gene and the *Escherichia coli LacZ* gene with a nuclear localization signal, both promoted by the cytomegalovirus promoter and flanked by AAV2 ITR sequences.

Cell culture. Human cervix epitheloid carcinoma (HeLa; ATCC CCL 2; American Type Culture Collection, Rockville, Maryland), mouse melanoma (B16F10), rat schwannoma (RN22; obtained from R. Timpl) and human coloncarcinoma (Co-115) cells have been described^{13,24}. They were maintained as monolayer cultures at 37 °C and 5% CO₂ in Dulbecco's modified Eagle's medium (DMEM) (HeLa, B16F10, RN22) or DMEM-Ham's-F12 (1:1) medium (Co-115) supplemented with 10% fetal calf serum (FCS), 100 U/ml penicillin, 100 µg/ml streptomycin and 2 mM L-glutamine.

Production of AAV2 particles. For the generation of AAV2 virions, HeLa cells were seeded at 10% confluency in plates 150 mm in diameter. Cells were transfected with DNA plasmids (35 µg pUC-AV2, pl-261, pl-381, pl-447, pl-534, pl-573 or pl-587 for the production of the wild-type AAV2, I-261, I-381, I-447, I-534, I-573 and I-587 AAV2 mutant viral preparations, respectively; or 17.5 µg pZnL with 17.5 µg of helper plasmid pRC or pRC(I-587) for the production of the rAAV/*LacZ* and rAAV(I-587)/*LacZ* AAV2-based viral vector preparations) by adding a 1:1 mixture of 2× BBS buffer (50 mM BES (N,N-bis(2-hydroxyethyl)-2-aminoethanesulfonic acid), pH 6.95, containing 280 mM NaCl, 0.75 mM Na₂HPO₄ and 0.75 mM NaH₂PO₄) and 260 mM CaCl₂ and subsequently incubated 18–22 h at 35 °C in an atmosphere of 3% CO₂. At 48 h after transfection, cells were incubated with adenovirus type 5 (multiplicity of infection = 5) for 1 h in 10 ml of serum-free medium and then supplemented with 10 ml of medium containing 20% FCS. At 72 h after adenovirus type 5 infection, the AAV2 viruses were purified and concentrated by two cycles of ultracentrifugation on CsCl gradients ($\rho = 1.4$ g/ml) as described²³.

Titer determination. The concentration of DNA containing viral particles was determined by DNA dot-blot hybridization. AAV2 viral preparations were first incubated with 500 µg/ml DNaseI to remove putatively free viral genomes that could be subsequently hybridized with the probe. The viral preparations were then blotted in serial dilutions and finally hybridized with a random-primed Rep probe by standard methods. Particle titers were determined by comparing the intensity of the hybridization signals with that obtained for a plasmid standard of known concentration blotted on the same membrane.

The titer was also tested by an ELISA using the mouse monoclonal antibody A20, which recognizes only assembled capsids of AAV2 (ref. 16). Purified A20 (200 ng) was attached to Costar microtiter plates by overnight incubation at 4 °C. After plates were blocked with PBS containing 10% bovine serum albumin (BSA) and 0.05% Tween 20, serial dilutions of AAV2 preparations were added to the wells, and were incubated for 3 h at room temperature. After washing with PBS, the wells were incubated with biotin-conjugated A20 for 1 h at room temperature. After a

second wash, the wells were incubated with peroxidase-conjugated streptavidin (Dianova Hamburg, Germany) for 1 h at room temperature. After plates were washed, 100 μ l of substrate solution (0.1 M sodium citrate buffer, pH 6.0, containing 0.1 μ g TMB (3,3',5,5'-tetramethylbenzidine) and 0.003% H₂O₂) was added to each well for 10 min, then the reaction was stopped by the addition of 50 μ l 1 M H₂SO₄. Light absorbance at 450 nm was then measured with an automated microplate reader (BioRad, Richmond, California). Particle titers were determined by comparing the absorbance with that obtained for viral preparation of known titer added to the same plate.

Detection of L14 peptide on capsid surface. To generate an antiserum against L14 peptide, a rabbit was injected intramuscularly with 250 μ g thyroglobulin-conjugated L14 peptide in Freund's complete adjuvant, and was then administered two booster injections at 3-week intervals with 200 μ g of thyroglobulin-conjugated L14 peptide in Freund's incomplete adjuvant. Blood was collected 1 week after the second booster injection, and serum was prepared by standard techniques.

An ELISA with antiserum against L14 was used to analyze the presentation of the L14 peptide on the capsid surface. Viral preparations (1×10^9 viral particles) were either directly coated in 100 μ l PBS on 96-well microtiter plates (Costar, Cambridge, Massachusetts) by overnight incubation at 4 °C (direct ELISA) or added to wells that had been coated with 200 ng A20 (indirect ELISA). Nonspecific binding was blocked with 100 μ l blocking buffer (PBS containing 10% bovine serum albumin and 0.05% Tween-20). Rabbit antiserum against L14 (diluted 1:1,000 in blocking buffer) was added to each well for 1 h at 37 °C. Plates were washed with PBS and subsequently incubated with biotin-conjugated goat antibody against rabbit (Dianova, Hamburg, Germany) for 1 h at 37 °C, and peroxidase-streptavidin for 1 h at room temperature. The colorimetric assay was done as for the A20 ELISA.

Cell attachment assay. Binding of the AAV2 mutants to the integrin receptor was analyzed in the cell attachment assay as described¹³. Viral preparations (1×10^9 viral particles) were coated directly onto 96-well microtiter plates in 100 μ l PBS and blocked in PBS containing 1% BSA. Cells (1×10^5 in 100 μ l) were plated in the coated plates and were allowed to attach for 30 min at 37 °C in a humidified incubator. At the end of the attachment period, the wells were washed twice with PBS to remove non-attached cells. Adherent cells were fixed with 100% ethanol (10 min), stained with crystal violet, washed extensively with distilled water, and the crystal violet was absorbed by the cells was solubilized with 0.5% Triton X-100 (50 μ l/well). Color yields were then measured at 570 nm with an ELISA reader. In the inhibition assays, cells were mixed with either RGDS or RGD soluble synthetic peptide at various concentrations (1–250 μ M) before adding to the plate.

Virus replication assay. Cells were grown to 70% confluency on slides and were infected with serial dilutions of viral preparations in serum-free medium containing adenovirus type 5 at a multiplicity of infection of 5 plaque-forming units per cell. In the inhibition assays, cells were infected in presence of 100 μ g/ml heparin or 200 μ M RGDS peptide. After a 1-hour incubation at 37 °C, the medium was replaced with fresh complete medium. Titers of viral preparations were determined 3 d later either by *in situ* detection of Rep protein synthesis in an immunofluorescence assay¹⁶ (Rep titer) or using the X-Gal *in situ* assay by cytochemical staining²³ (LacZ titer). Titers were calculated from the last limiting dilution of viral stocks that led to fluorescence-positive cells or to β -galactosidase-producing cells, respectively.

Acknowledgments

We thank I. Renner-Müller and E. Wolf for their help and providing their animal facilities to produce rabbit antiserum against L14. This work was supported by grants from the Wilhelm-Sanderstiftung, Bayerische Forschungsförderung, and the Deutsche Forschungsgemeinschaft (Sonderforschungsbereich 455) (M.H. and A.G.) and stipends of the Studienstiftung des Deutschen Volkes and the Fond der Chemischen Industrie (BMBF) (M.R.).

RECEIVED 1 MARCH; ACCEPTED 7 JULY 1999

- Kotin, R.M. Prospects for the use of adeno-associated virus as a vector for human gene therapy. *Hum. Gene Ther.* **5**, 793–801 (1994).
- Hallek, M. *et al.* Recombinant adeno-associated virus vectors. *IDrugs* **1**, 561–573 (1998).
- Mizukami, H., Young, N.S. & Brown, K.E. Adeno-associated virus type 2 binds to a 150-kilodalton cell membrane glycoprotein. *Virology* **217**, 124–130 (1996).
- Summerford, C. & Samulski, R.J. Membrane-associated heparan sulfate proteoglycan is a receptor for adeno-associated virus type 2 virions. *J. Virol.* **72**, 1438–1445 (1998).
- Summerford, C., Bartlett, J.S. & Samulski, R.J. $\alpha\beta 5$ integrin: a co-receptor for adeno-associated virus type 2 infection. *Nature Med.* **5**, 78–82 (1999).
- Qing, K. *et al.* Human fibroblast growth factor receptor 1 is a co-receptor for infection by adeno-associated virus 2. *Nature Med.* **5**, 71–77 (1999).
- Hermonat, P.L., Labow, M.A., Wright, R., Berns, K.I. & Muzyczka, N. Genetics of adeno-associated virus: isolation and preliminary characterization of adeno-associated virus type 2 mutants. *J. Virol.* **51**, 329–339 (1984).
- Tratschin, J.D., Miller, I.L. & Carter, B.J. Genetic analysis of adeno-associated virus: properties of deletion mutants constructed in vitro and evidence for an adeno-associated virus replication function. *J. Virol.* **51**, 611–619 (1984).
- Ruffing, M., Heid, H. & Kleinschmidt, J.A. Mutations in the carboxy terminus of adeno-associated virus 2 capsid proteins affect viral infectivity: lack of an RGD integrin-binding motif. *J. Gen. Virol.* **75**, 3385–3392 (1994).
- Tsao, J. *et al.* The three-dimensional structure of canine parvovirus and its functional implications. *Science* **251**, 1456–1464 (1991).
- Geourjon, C. & Deléage, G. OPM: a self-optimized method for protein secondary structure prediction. *Protein Eng.* **7**, 157–164 (1994).
- Thompson, J.D., Higgins, D.G. & Gibson, T.J. CLUSTAL W: improving the sensitivity of progressive multiple sequence alignment through sequence weighting, position-specific gap penalties and weight matrix choice. *Nucleic Acids Research* **22**, 4673–4680 (1994).
- Aumailley, M., Gerl, M., Sonnenberg, A., Deutzmann, R. & Timpl, R. Identification of the Arg-Gly-Asp sequence in laminin A chain as a latent cell-binding site being exposed in fragment P1. *FEBS Lett.* **262**, 82–86 (1990).
- White, J.M. Integrins as virus receptors. *Curr. Biol.* **3**, 596–599 (1993).
- Valsesia-Wittmann, S. *et al.* Modifications in the binding domain of avian retrovirus envelope protein to redirect the host range of retroviral vectors. *J. Virol.* **68**, 4609–4619 (1994).
- Wüstuba, A., Kern, A., Weger, S., Grimm, D. & Kleinschmidt, J.A. Subcellular compartmentalization of adeno-associated virus type 2 assembly. *J. Virol.* **71**, 1341–1352 (1997).
- Stewart, P.L. *et al.* Cryo-EM visualization of an exposed RGD epitope on adenovirus that escapes antibody neutralization. *EMBO J.* **16**, 1189–1198 (1997).
- Yang, Q. *et al.* Development of novel cell surface CD34-targeted recombinant adeno-associated virus vectors for gene therapy. *Hum. Gene Ther.* **9**, 1929–1937 (1998).
- Bartlett, J.S., Kleinschmidt, J.A., Boucher, R.C. & Samulski, R.J. Targeted adeno-associated virus vector transduction of nonpermissive cells mediated by a bispecific F(ab')₂ antibody. *Nat. Biotech.* **17**, 181–186 (1999).
- Smith, T.F. & Waterman, M.S. Identification of common molecular subsequences. *J. Mol. Biol.* **147**, 195–197 (1981).
- Kabsch, W. & Sander, C. Dictionary of protein secondary structure: pattern recognition of hydrogen-bonded and geometrical features. *Biopolymers* **22**, 2577–2637 (1983).
- Samulski, R.J., Chang, L.S. & Shenk, T. A recombinant plasmid from which an infectious adeno-associated virus genome can be excised in vitro and its use to study viral replication. *J. Virol.* **61**, 3096–3101 (1987).
- Chiorini, J.A. *et al.* High-efficiency transfer of the T cell co-stimulatory molecule B7-2 to lymphoid cells using high-titer recombinant adeno-associated virus vectors. *Hum. Gene Ther.* **6**, 1531–1541 (1995).
- Carrel, S., Sordat, B. & Merenda, C. Establishment of a cell line (Co-115) from a human colon carcinoma transplanted into nude mice. *Cancer Res.* **36**, 3978–3984 (1976).

Copyright of Nature Medicine is the property of Nature Publishing Group and its content may not be copied or emailed to multiple sites or posted to a listserv without the copyright holder's express written permission. However, users may print, download, or email articles for individual use.